

U-GROOVE ALUMINUM WELD STRENGTH IMPROVEMENT

V. Verderaine* and R. Vaughan*

NASA Marshall Space Flight Center, Alabama, 35812

Abstract

Though butt-welds are among the most preferred joining methods in aerospace structures, their strength dependence on inelastic mechanics is generally the least understood. This study investigated experimental strain distributions across a thick aluminum U-grooved weld and identified two weld process considerations for improving the multipass weld strength. The extreme thermal expansion and contraction gradient of the fusion heat input across the groove tab thickness produces severe peaking which induces bending under uniaxial loading. The filler strain-hardening decreased with increasing filler pass sequence, producing the weakest welds on the last pass side. Current welding schedules unknowingly compound these effects which reduce the weld strength. A de-peaking index model was developed to select filler pass thicknesses, pass numbers, and sequences to improve de-peaking in the welding process. Intent is to combine the strongest weld pass side with the peaking induced bending tension to provide a more uniform stress and stronger weld under axial tensile loading.

N = axial load variable
 p = inelastic variable
 tu = tensile ultimate
 ty = tensile yield

I. Introduction

As structural environments and component sizes increase, butt-weld thicknesses increase, weld development and processes become more complex, and joint strengths are less predictable. One early study¹ modeled a uniaxial butt-weld specimen having different inelastic lateral contraction rates between pre-weld material and weld filler and discovered a metallurgical discontinuity at the interfaces. Discontinuity stresses, especially transverse shear, were later experimentally verified² on a thick weld cross section in uniaxial test. This study further explored the multipass welding process and resulting structural properties of weld filler passes from experimental test data,³ and identified weld process variables that should improve strength performance.

Nomenclature

E = elastic modulus, ksi
 F = material strength, ksi
 H = specimen thickness, inch
 h = weld pass thickness, inch
 K = inelastic strength coefficient, ksi
 M = induced moment, inch-kips
 N = applied axial load, kips
 n = strain-hardening exponent,
total number of weld passes
 m = weld sequence number
 T = temperature, °F
 t = U-groove tabs thickness, inches
 w = specimen width, inch
 α = coef. of thermal expansion, in/in/°F

Subscripts

α = thermal variable
 e = elastic variable
 i = strain gage number,
weld pass series
 j = weld pass number
 k = designated temper
 M = moment variable

II. Weld peaking specimen

The aluminum test specimen shown in figure 1 was a double U-grooved butt-weldment of two machined 2219 panels. The weld filler was 2319 aluminum with the beads ground off. The Specimen was 1.4 inches thick and 0.71 inches wide, and the butted tab thickness between the double U-grooves was 0.375 inches. It was TIG welded using a normal welding schedule. The butted tabs were tack and continuous fusion welded from the same side, incurring a net initial peaking angle ϕ_2 . Weld peaking is an unintentional angular panel displacement resulting from weld thermal gradient strain. Subsequent welds were filler passes serially applied, first in the groove opposite pass #1 and 2, and then on the reverse side groove for a total of eight passes.

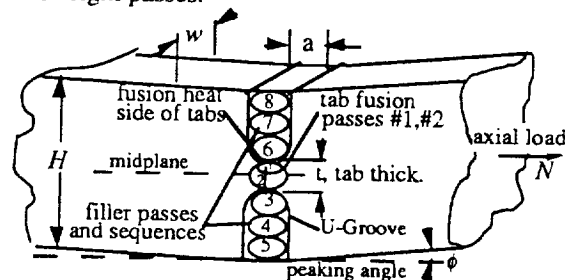


Fig. 1. Test specimen configuration

Weld pass #1 in figure 1 was crucial to the butted edge mismatch. In this weld pass, the double U-groove tabs at the midplane were butted, the panel surface planes were aligned, the assembly was constrained, and the butted tabs were fusion tack welded (without filler material) on

* Aerospace Engineers, Structures and Dynamics Laboratory

one side. The tack weld pass produced local thermal expansion on the butted tabs and was followed by cooling contraction. The cooling induced a tensile strain on the tack weld side and compression on the unfused side of the tab, which mildly peaked the panels with the obtuse angle on the tack welded (pass #1) side.

The intense weld heat input from pass #2 severely increased the adverse peaking angle. It was another fusion weld pass applied on the same side of the tack weld, and it had the highest heat input rate to fuse the total tab thickness. The associated extreme thermal expansion and contraction gradient across the tab thickness produced the maximum peaking angle in the process with the obtuse angle again on the heat source side (#1 pass).

The next three passes were weld filler passes (thinner than the tabs) requiring less heat and were applied in the groove opposite the #1 tack pass side. Each weld pass produced a thermal gradient and expansion across the welded section. Upon cooling, the filler pass contracted inelastically and then elastically in tension, which bent and strain hardened the tabs and the built-up filler passes. These passes reduced the peaking angle (de-peaking) produced by the two fusion weld passes. Subsequent weld passes were applied on the opposite groove, producing less thermal straining, and moderately increasing the weld peaking.

III. De-peaking model

The extent of peaking at any point in the process depended on the initial peaking from the fusion passes and the de-peaking and peaking contributions of successive filler weld passes. Increasing the laid-up weld thickness increases the section modulus, which stiffens and reduces the panel deflection rate induced by the succeeding thermally contracted filler passes. It then follows that successive thermal bending and strain-hardening decrease, and that the net de-peaking angle is governed by the groove side accumulating the most and earliest thermal tensile straining. Therefore, the peaking angle ϕ_m , for any pass $j > 2$ and at the m -th sequence in the welding process, may be expressed by

$$\phi_m = \phi_2 + \sum_{j=3}^m s_j \phi_j \quad (1)$$

where the first term is the initial peaking angle ($\phi_2 > \phi_3$) produced by the fusion welds on the U-groove tabs. The second term is the sum of subsequent de-peaking and peaking weld passes for $j \geq 3$. The coefficient "s" polarizes the weld pass sequence where $s = +1$ refers to the peaking weld pass applied in the groove on the weld pass #1 side of the specimen, and $s = -1$ refers to the de-peaking pass applied in the opposite groove.

Figure 2 qualitatively modeled the weld peaking behavior of the j -th pass in the welding process. The peaking angle ϕ at the j -th weld pass was derived with designer control variables, which are the weld pass

thicknesses, h_i , the polarity, and the accumulated thickness. Passive control variables, such as material constants and unique coefficients, were lumped into unquantified coefficients leading to versatile qualitative expressions.

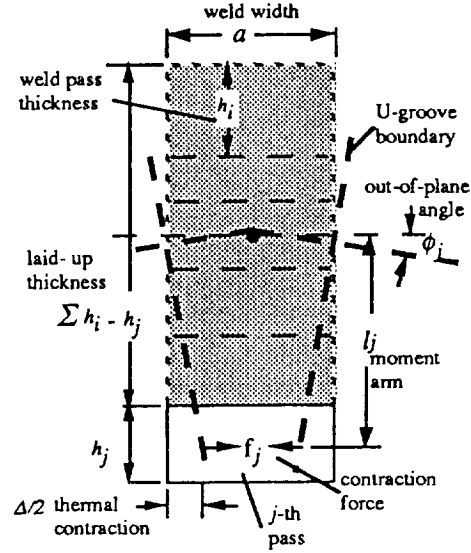


Fig. 2. Peaking from j -th filler pass

The cooling contraction of the j -th weld pass induces a tensile force of

$$f_j = \sigma_\alpha h_j \quad (2)$$

where the thermal stress is derived from the filler thermal contraction equated to the stress tension displacement,

$$\Delta = a \alpha T = a \frac{\sigma_\alpha}{E}$$

and is reduced to

$$\sigma_\alpha = \alpha E T \quad (3)$$

Substituting Eq. (3) and the moment arm in Fig. 2 into Eq. (2), the moment imposed by the thermal contraction force about the accumulated weld passes centroid is

$$M_j = f_j s_j \left[\frac{1}{2} \sum_{i=1}^j h_i \right] = \frac{1}{2} \alpha E T s_j h_j \sum_{i=1}^j h_i \quad (4)$$

and the resulting peaking angle of the stub filler section was approximated by a third degree stress function⁴

$$\phi_j = \frac{c_1 M_j a}{E \left(\frac{1}{2} \sum_{i=1}^j h_i - h_j \right)^3} \quad (5)$$

Substituting Eq. (4) into Eq. (5), the peaking angle induced by the j -th weld pass is

$$\phi_j = \frac{c s_j h_j \sum_{i=1}^j h_i}{\left(\sum_{i=1}^{j-1} h_i\right)^3} \quad (6)$$

Substituting Eq. (6) into the second term of Eq. (1), the de-peaking angle at the end of the m -th sequence is given by

$$\phi_{m>2} = \phi_m - \phi_2 = \sum_{j=3}^m s_j \phi_j = c \alpha Z_{m>2},$$

where the desired de-peaking index is expressed by

$$Z_{m>2} = \sum_{j=3}^m \frac{s_j h_j \sum_{i=1}^j h_i}{\left(\sum_{i=1}^{j-1} h_i\right)^3} \quad (7)$$

The de-peaking index of Eq. (7) was applied to the normal welding schedule of figure 1, having a uniform filler weld pass thickness of

$$h_i = \frac{(H-t)}{n-2} = \frac{(1.4 - 0.375)}{8-2} = 0.171.$$

Substituting the uniform filler thickness into Eq. (7), the de-peaking index after the $m = 5$ pass is

$$Z_5 = -\frac{.17(.375+.17)}{(.375)^3} - \frac{.17(.375+2(.17))}{(.375+.17)^3} - \frac{.17(.375+3(.17))}{(.375+2(.17))^3} = -3.34,$$

and after $m = n = 8$ is

$$Z_8 = Z_5 + 0.56 = -2.78.$$

De-peaking indices after each filler pass are listed in table 1 for centered tabs and a normal weld schedule. Since the specimen showed a peaking angle of 0.02 radians, the peaking index may be assumed to be $Z_{2>} + 2.8$ and the normal weld schedule proved to be insufficient. In another case, the U-groove tabs were assumed off-centered by one pass of the same filler pass thickness to provide an additional de-peaking weld pass within the specimen thickness. The de-peaking index increased to -3.3, which might have reversed the weld peaking side.

Table 1. De-peaking indices at weld sequences

Weld sequence, m	3	4	5	6	7	8
Centered tab, Z	-1.7	-2.5	-3.3	-3.1	-2.9	-2.7
Off-cent., tab Z	-1.7	-2.5	-3.3	-3.6	-3.4	-3.3

Other weld schedule options with centered tabs were assessed through Eq. (7). Increasing the welds to 4 thinner filler passes on the peaking side for a total of 9

filler passes provided an index of -2.82, and no improvement over the normal weld schedule. Increasing the weld passes to 10 uniform filler thicknesses provided a worse index of -1.9.

IV. Weld test data

The complex thermal straining, work-hardening, and annealing environments experienced by each unique weld pass posed the question of how unique their structural properties might be after the final heat treatment. Reference 3 provided the necessary experimental strain data of the instrumented specimen shown in Fig. 3. A total of 5 equidistant electrical strain gages was oriented to obtain axial strain measurements along the specimen thickness under uniaxial loading.

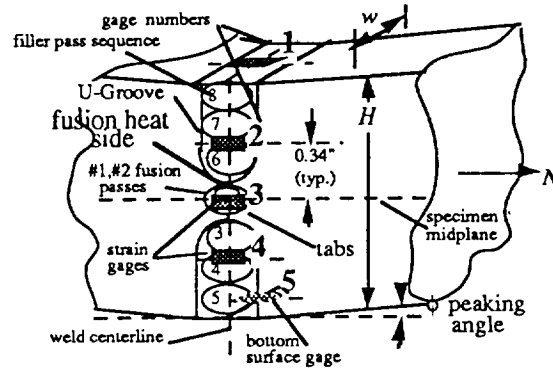


Fig. 3. Strain instrumentation

Surface mounted gages #1 and #5 measured strains from weld passes #8 and #5, respectively, of the normal welding schedule. Gage numbers 2, 3, and 4 measured average strains from pairs of weld pass numbers 7 and 6, 1 and 2, and 3 and 4, respectively. Table 2. provided the experimental³ strain gage data as a function of incrementally applied axial loads.

Table 2. Experimental weld strains, 10^{-3} in/in

Gage Nos.	Loads, N , kips						
	5	10	15	20	25	30	35
1	0.8	1.5	2.6	4.0	6.3	10.4	19.0
2	0.5	1.0	1.6	2.4	3.4	5.6	11.8
3	0.4	0.9	1.4	2.0	2.8	4.0	7.0
4	0.4	0.8	1.3	1.8	2.6	3.7	7.0
5	0.4	0.6	1.0	1.2	1.6	2.0	3.2

Figure 4 illustrates the measured strain distributions along the weld filler cross section, using table 2 data. At loads less than 15 kips, strains are seen to produce planes of uniformly varying strains along the cross section that are indicative of elastic bending of a homogeneous material. Inelastic strain responses are spotted by the onset change of constant strain rate to a suddenly increased rate under constant loading rate. The inelastic strains are noted to not conform into planes for

common steps of axial loading, which clearly denotes zones of nonhomogeneous filler materials.

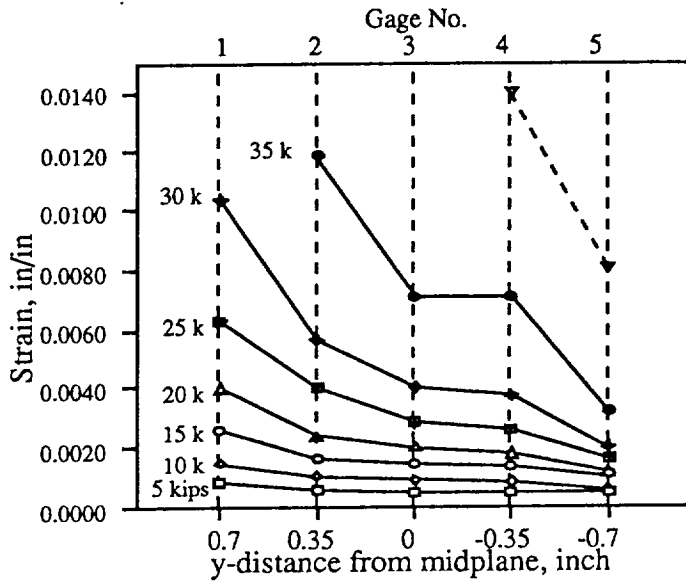


Fig. 4. Strain distribution across thickness

This onset of inelastic strain behavior of each weld pass under constant load rate signifies a unique filler pass property which may be estimated from materials and load equilibrium models.

V. Weld filler properties

Modeling elastic-inelastic behavior could be very difficult⁵ unless idealized into the simplest mathematical expressions within the physical phenomena of the material and its application. The uniaxial stress-strain relationship of a polycrystalline material may be appropriately represented by the power expression,⁶

$$\sigma = K \epsilon^n \quad (8)$$

requiring no interpretation through theory. The strain-hardening exponent, "n" is the log-log slope of Eq. (8) and is defined by $n = 1$ in the elastic region when $\sigma \leq F_{ty}$.

Many mechanical properties of aluminum are seen to be related by their common face-centered-cubic lattice substructure and copper alloy. They all have a common elastic modulus of $E = 10500$ ksi, and all demonstrate similar strain-hardening curves. Their strength dispersions are fixed by their temper processes which establish their unique elastic stress limit and strain-hardening slope. Therefore, it is not surprising that the inelastic stress-strain slopes of any temper "k" are noted⁷ to vary linearly with yield stresses. Given the yield stress of any temper, the strain-hardening exponent (slope) may be shown to be approximated (within 5 percent) by the linear expression

$$n_k = 0.34 - 0.0045 F_{ty, k} \quad (9)$$

The strength coefficient "K" is evaluated at the elastic-inelastic material interface, which is the yield stress, and the coefficient is expressed by

$$K = E^n F_{ty}^{(1-n)} \quad (10)$$

Thus, determining the experimental yield stress, the Eq. (8) inelastic parameter of each weld pass may be derived through Eqs. (9) and (10).

Because of peaking induced bending, the onset of yield strain is a serendipity observed in Fig. 4 to emerge at one gage per each sequentially and successively increased interval of axial loading. Then, for each interval of applied loading, the portion of that load imposed on each gage region is expressed by the product of that proportional area and Eq. (8) with the measured strain. Their sum for that interval are equated to the external-internal load equilibrium formula

$$N = wh (\Sigma K \epsilon_p^n p + E \Sigma \epsilon_e p) \quad (11)$$

from which each material set of parameters are calculated through Eqs. (9) and (10) through each increasing interval of applied loading.

Terms on the right of the equation are the sum of inelastic and elastic internal loads calculated from their measured strains, respectively. The weld pass thickness was assumed to be equally divided along the thickness for an average of $h = H/8 = 0.175$ inches, and "p" is the number of passes represented by each respective strain gage. This technique was applied to all five strain gage data to identify and define weld pass inelastic properties along the weld centerline.

In determining filler properties from strains induced at load $N = 15$ kips, at least one strain had to be inelastic to not exceed the load equilibrium of Eq. (11). That inelastic strain had to be on the verge of a strain rate increase, such as gage #1 measuring $\epsilon_I = 0.0026$. Substituting the inelastic and all elastic strains induced at $N = 15$ kips into Eq. (11),

$$pK(.0026)^n = \frac{15}{0.124} - 10500(.001 + 2(.0016 + .0014 + .0013))$$

where $p=1$, the inelastic stress was,

$$K(.0026)^n = 20.2 \text{ ksi} \quad (12)$$

By trial (or Newton method), a yield stress was selected and applied into Eqs. (9) and (10) to satisfy Eqs. (8) and (12). Resulting properties representing weld pass #8 were listed in table 3. At 20 kips loading, the inelastic weld pass properties to be determined were passes #6 and #7 represented by gage #2. Substituting the above derived

inelastic properties of weld pass #8 in Eq. (8) and continuing as with the 15 kips loading case, the load equilibrium of Eq. (11) was

$$2K(.0024)^n = \frac{20}{0.124} - 94.7(.004)^{0.254} - 10500(.0012 + 2(.002 + .0018)) ,$$

and the inelastic stress was $K(.0024)^n = 22.8$ ksi .

Results from similarly derived inelastic properties at all other strain gages along the weld center line are also listed in table 3.

Table 3. Weld filler inelastic properties

Gage Nos	1	2	3	4	5
Weld pass #	8	7.6	1.2	3.4	5
F_{ty} ksi	19	22	27	37	30
n	0.245	0.241	0.218	0.174	0.205
K ksi	94.7	97.3	99.3	98.6	99.7
σ_{ϕ} ksi	46	49	53	58	56
ϵ_{ty}	.0018	.0021	.0025	.0035	.0028

Though listed results from Eq. (11) confirmed the suspected variation of inelastic properties among the weld passes, the orderly decrease of filler yield stress unexpectedly correlated with the orderly increase in weld pass sequence. The last weld pass #8 at gage #1 was noted to have the lowest yield property, the prior pass had the next lowest yield property, and etc. This phenomenon was verified by an independent graphic analysis producing the same results.

Decreasing filler pass yield stress with increasing sequence pass is a particularly interesting phenomenon in that it coincides with the decreasing peaking index of Eq. (7). Since weld de-peaking and strain-hardening decreases with increasing passes, later filler passes experience less strain-hardening and, therefore, acquire less heat treatment and lower yield stress. Consequently, if the weaker last pass filler (on obtuse angle side of the specimen) is combined with the tension component of the induced moment, the last pass filler will prematurely rupture under uniaxial loading.

A more significant weld strength improvement would be to de-peak the weld sufficiently to reverse the obtuse angle on the first pass side in order to induce the tension component of the peaking moment on the earlier passes having higher yield stresses and strength. This process would provide a more uniform stress across the weld thickness, producing a stronger weld in axial tension.

VI. Conclusions

Weld fillers, having the lowest elastic limit and limited width, will yield first and progressively distort most in bending. This principle was especially appreciated in weld strength reduction of multipass welds leading to this study on the influences of peaking.

A de-peaking index model was developed for a double U-grooved weldment that denoted the groove side receiving the thicker and most filler passes earliest produced the greater de-peaking angle. A large range of de-peaking angles may be achieved through the welding process selection of designer control parameters, such as filler pass thickness, number of passes, and polarities.

Using experimental strain data from a double U-groove aluminum weldment, the filler pass inelastic properties were noted to vary across the weld thickness with the weld filler yield stress decreasing with increasing sequence number. This phenomenon coincided with the decreasing peaking index model, in which strain-hardening decreases with increasing passes, and acquires less heat treatment producing lower yield stress.

Consequently, if the weaker last pass filler (obtuse angle side of the specimen) is combined with the tension component of the induced bending, the last pass filler will prematurely rupture under uniaxial loading. Then, obviously, it is not sufficient to reduce the peaking angle through normal weld schedules and planishing, but the angle must be reversed.

An enhanced welding schedule would de-peak the weld sufficiently to reverse the obtuse angle to the first pass side in order to impose the tension component of the induced bending on the earlier weld passes having higher yield and ultimate strengths. Reversing the weld peaking provides a more uniform and lower stress across the weld thickness, resulting in a stronger tensile joint. This simple innovation may be the least intrusive modification on current and future structural productions.

Acknowledgment: The authors appreciate the review comments by Mr. Dennis Moore and are grateful to Dr. Jim Blair for this assigned opportunity and for his remarks and usual professional support.

REFERENCES

1. Verderame, V.: "Plate and Butt-Weld Stresses Beyond Elastic limits", NASA TP-3075, Jan. 1991.
2. Kerkof, S.: "AFT Skirt Weld Analysis Methods," United Technology, USBI, presentation to MSFC, April 16, 1991.
3. Gambrell, S.: "Use of Photostress and Strain Gages to Analyze Behavior of Weldments", NASA/MSFC Contract No. NAG 8-293, Sub 93-101, Univ. of AL, Tuscaloosa AL, 1993.
4. Timoshenko, S. and Goodier, J.: "Theory of Elasticity," McGraw-Hill Book Co., 1951.
5. Phillips, A.: "Introduction to Plasticity", The Ronald Press Company, 1956.
6. Dieter, G.: "Mechanical Metallurgy", 3rd edition, McGraw-Hill, Inc., N.Y., 1986.
7. Anon., MIL-Handbook C5: "Metallic Materials and Elements for Aerospace Vehicle Structures," September 1976.